



HAL
open science

Dynamic full-field optical coherence tomography as complementary tool in fungal diagnostics

Thomas Maldiney, Jean-Marie Chassot, Claude Boccara, Mathieu Blot, Lionel Piroth, Pierre-Emmanuel Charles, Dea Garcia-Hermoso, Fanny Lanternier, Frédéric Dalle, Marc Sautour

► To cite this version:

Thomas Maldiney, Jean-Marie Chassot, Claude Boccara, Mathieu Blot, Lionel Piroth, et al.. Dynamic full-field optical coherence tomography as complementary tool in fungal diagnostics. Journal of Medical Mycology = Journal de Mycologie Médicale, 2022, 32 (4), pp.101303. 10.1016/j.mycmed.2022.101303 . pasteur-04173114

HAL Id: pasteur-04173114

<https://pasteur.hal.science/pasteur-04173114v1>

Submitted on 22 Jul 2024

HAL is a multi-disciplinary open access archive for the deposit and dissemination of scientific research documents, whether they are published or not. The documents may come from teaching and research institutions in France or abroad, or from public or private research centers.

L'archive ouverte pluridisciplinaire **HAL**, est destinée au dépôt et à la diffusion de documents scientifiques de niveau recherche, publiés ou non, émanant des établissements d'enseignement et de recherche français ou étrangers, des laboratoires publics ou privés.



Distributed under a Creative Commons Attribution - NonCommercial 4.0 International License

Dynamic Full-Field Optical Coherence Tomography as Complementary Tool in Fungal Diagnostics

1 **Thomas Maldiney^{1,2*}, Jean-Marie Chassot³, Claude Boccara³, Mathieu Blot^{2,4}, Lionel**
2 **Piroth^{4,5}, Pierre-Emmanuel Charles^{2,6}, Dea Garcia-Hermoso⁷, Fanny Lanternier^{7,8},**
3 **Frédéric Dalle^{9,10}, Marc Sautour^{9,10}**

4 ¹Department of Intensive Care Medicine, William Morey General Hospital, Chalon-sur-
5 Saône, France

6 ²Lipness team, INSERM Research Center LNC-UMR1231, University of Burgundy, Dijon,
7 France

8 ³Institut Langevin, ESPCI Paris, PSL University, CNRS, 75005 Paris, France

9 ⁴Infectious Diseases Department, Dijon Bourgogne University Hospital, Dijon, France

10 ⁵INSERM, CIC1432, Clinical Epidemiology unit, Dijon, France

11 ⁶Department of Intensive Care, Dijon Bourgogne University Hospital, Dijon, France

12 ⁷Institut Pasteur, Université de Paris, Molecular Mycology Unit, National Reference Center
13 for Invasive Mycoses and Antifungals (NRCMA), UMR 2000, CNRS, Paris, France

14 ⁸Department of Infectious Diseases and Tropical Medicine, Necker-Enfants Malades Hospital,
15 Assistance Publique-Hôpitaux de Paris, Paris, France

16 ⁹Department of Parasitology/Mycology, Dijon Bourgogne University Hospital, 21000 Dijon,
17 France

18 ¹⁰UMR PAM A 02.102 Procédés Alimentaires et Microbiologiques, Univ. Bourgogne
19 Franche-Comté, AgroSup Dijon, Dijon, France

20 *** Correspondence :**
21 thomas.maldiney@ch-chalon71.fr

22 **Keywords: Full-Field Optical Coherence Tomography, Fungal Diagnostics, Invasive**
23 **Fungal Infections, Dynamic Contrast, Fungal Metabolism.**

24 **Abstract**

25 Histopathology and microscopic examination of infected tissue are the gold standards to
26 prove the diagnosis of invasive fungal infection (IFI). Yet, they suffer from essential
27 limitations that hamper rapid diagnosis and require the future development of new imaging
28 tools dedicated to fungal diagnostics. To this end, the present work introduces the first use of
29 dynamic full-field optical coherence tomography (D-FF-OCT) for the visualization of
30 microscopic filamentous fungi. Data collected from the observation of three different fungal
31 species (*Nannizzia gypsea*, *Aspergillus fumigatus* and *Rhizopus arrhizus*) confirm the ability
32 of D-FF-OCT to visualize not only the main structures of all selected fungal species (hyphae,
33 spores, conidia, sporulating structures), but also the metabolic activity of the organisms,
34 which could provide additional help in the future to better characterize the signature of each
35 fungal structure. These results demonstrate how D-FF-OCT could serve as potential
36 complementary tool for rapid diagnosis of IFI in both intensive and non-intensive care units.

37 1 Introduction

38 Invasive fungal infections (IFI) are associated with a large morbi-mortality in both
39 immunocompromised and critically ill patients [1,2]. According to a recent update from the
40 European Organization for Research and Treatment of Cancer and the Mycoses Study Group
41 Education and Research Consortium (EORTC/MSGERC), IFI diagnosis mostly relies on the
42 combination of host factors, clinical features, as well as mycological evidence [3]. Indeed,
43 despite tremendous progress regarding the validation and implementation of polymerase chain
44 reaction (PCR)-based methods as essential criteria for probable invasive fungal disease,
45 histopathology or microscopic examination of infected tissue remain gold standards for the
46 diagnosis of proven IFI [4,5]. Yet, the absolute necessity to obtain a timely and proven
47 diagnosis in specific cases of IFI requires to address many challenges and pitfalls in
48 histopathology or other culture-independent solutions dedicated to the diagnosis of fungal
49 diseases [6]. As an example, a convenient tool to allow a rapid and easy differential diagnosis
50 between invasive aspergillosis and mucormycosis *in situ* would help both infectious disease
51 specialists and surgeons to choose the best therapeutic option between exclusive medical
52 treatment and the adjunction of urgent extensive surgery. One of the solutions would be to
53 uncover a technology able to assess the invasive nature of a fungal species within one
54 superficial or deep tissue sample in a few minutes only, and without any coloration step.

55 As full-field optical coherence tomography (FF-OCT), dynamic full-field optical coherence
56 tomography (D-FF-OCT) relies on broad band interference microscopy and provides ultra-
57 high resolution structure images of biological tissues [7] as well as subcellular metabolic
58 contrast within a few minutes [8]. In comparison to standard OCT or confocal microscopy, D-
59 FF-OCT was shown to improve spatial resolution up to ten times [9]. Apart from recent
60 medical applications [7,10,11], most studies have considered the potential importance of D-
61 FF-OCT as imaging alternative for extemporaneous analysis in oncologic interventions and
62 future way to easier and quicker surgical pathology [12]. However and excluding previous
63 attempts to visualize *Malassezia* Folliculitis [13], cutaneous larva migrans [14] and even
64 *Sarcoptes scabiei* infestation [15] with OCT systems displaying neither high spatial resolution
65 nor the ability to follow dynamic contrast, there has been to our knowledge no reported
66 attempt to exploit high-definition D-FF-OCT in fungal diagnostics. The present work
67 introduces the first application of D-FF-OCT for the observation of different filamentous
68 fungal species *in vitro*. We address the hypothesis that D-FF-OCT could help both physicians
69 and pathologists to circumvent common pitfalls and develop timely and automated
70 histopathology analysis dedicated to the diagnosis of IFI.

71 2 Materials and Methods

72 2.1 Fungal strains

73 *Nannizzia gypsea* (NG), *Aspergillus fumigatus* (AF) and *Rhizopus arrhizus* (RA) were
74 isolated from patients and identified by mass spectrometry (MALDI-TOF) in the laboratory of
75 Parasitology-Mycology of Dijon Bourgogne University Hospital. The strains were cultivated
76 on Sabouraud dextrose agar (BioMérieux SA, Marcy-l'Etoile, France) and incubated at 28°C
77 for proper growth.

78 2.2 FF-OCT standard and dynamic contrast imaging

79 As described elsewhere [10] and presented in Figure 1, D-FF-OCT images were acquired with
80 a commercially available D-FF-OCT apparatus (Light-CTScanner, LLTech - Aquyre

81 Bisciences, Paris, France) [16]. Briefly, a conventional halogen source with short temporal
82 coherence length was used for illumination to ensure an axial resolution of 1 μm (Figure 1A).
83 As for the previously reported D-FF-OCT set-up, 10x water immersion microscope objectives
84 were placed in the interferometer arms (Linnik configuration) to reach a transverse resolution
85 of approximately 1.5 μm . Solid cultures (Figure 1B) were sampled and deposited on the upper
86 slide of the apparatus sample holder according to an adapted protocol based on the tape touch
87 method described elsewhere for fungal slide mounts [17]. The resulting fungal slides were
88 then acquired following full-field illumination and subsequent dynamic contrast imaging with
89 a complementary metal oxide semiconductor camera (Figure 1C). The penetration depth was
90 adjusted to be approximately 100 μm and series of D-FF-OCT images with 1.5 μm spacing
91 were recorded in depth.

92 **2.3 Image analysis**

93 ImageJ 1.49k software was used for axial z-stacking of multiple images and three-
94 dimensional reconstruction (3D viewer plugin). Both FF-OCT standard and dynamic contrast
95 image analysis with length measurements of different fungal compartments for each selected
96 species were accessible using a contrast-based ImageJ 1.49k protocol called the “Plot Profile”
97 Function. Regarding the specific analysis of dynamic contrast images, the time series
98 associated to each pixel behavior was analyzed by a fast Fourier transform program. Then the
99 spectrum was divided in three parts respectively associated to the three colors of the
100 composite RGB images so that the highest frequencies (fast movements) correspond to the red
101 color and the lowest frequencies to the bluer colors.

102 **3 Results**

103 **3.1 D-FF-OCT observations of *Nannizzia gypsea***

104 The different aspects of NG are displayed in Figure 2. The two-dimensional structural FF-
105 OCT image of NG from Figure 2A returns multiple thin and septate hyphae, most of the time
106 longer than 200 μm , with a diameter ranging from 2 to 4 μm . Except for septa, the intensity of
107 the FF-OCT signal is relatively comparable on the whole hyphae. The dynamic D-OCT image
108 from Figure 2B confirms a similar shape of the NG hyphae with a homogenous and rather low
109 dynamic contrast, from blue to pale green, no matter which septum of the septate hyphae.
110 Three dimensional FF-OCT image of both hyphae and multicelled macroconidia are shown in
111 Figure 2C. Macroconidia appear as fusiform structures approximately 50 μm -long and 15 μm -
112 large with distinguishable septa (Figure 2C, white arrow). When compared to the bluish
113 dynamic aspect of NG hyphae from Figure 2B, dynamic D-OCT image from Figure 2D shows
114 intense orange dynamic contrast within the macroconidia of NG and outlines its multicelled
115 structure.

116 **3.2 D-FF-OCT observations of *Aspergillus fumigatus***

117 Acquisitions of AF solid cultures with D-FF-OCT are shown in Figure 3. As demonstrated by
118 the two-dimensional image from Figure 3A, AF is composed of several septate conidiophores
119 with length ranging from 200 to 300 μm and a diameter of 4-6 μm , slightly larger than the one
120 from NG. When compared to the different compartments of NG, Figure 3A confirms a
121 different FF-OCT signal between conidiophores, vesicles, phialides and conidia. The latter,
122 with the smallest diameter of 2-4 μm , clearly show the brightest FF-OCT signal in
123 comparison to the other parts of AF, notably vesicles. The two-dimensional dynamic D-OCT
124 image displayed in Figure 3B highly contrasts with the corresponding structure image
125 acquired with FF-OCT. Although the different sub-compartments display a morphology

126 comparable to the one from Figure 3A, both dynamic contrast and intensity enlighten
127 complementary signature of each structure. First, the dynamic contrast can vary from pale
128 blue to green or even yellow from one side of a conidiophore to another. In addition, vesicles
129 most often display bright green-orange dynamic contrast, as compared to the pale bluish
130 colors of the conidial heads or phialides. Finally, we see from Figure 3C that three-
131 dimensional dynamic D-OCT image confirms the whole structure and dynamic contrast of
132 both the conidiophores and conidial heads, approximately 50 μm -large.

133 3.3 D-FF-OCT observations of *Rhizopus arrhizus*

134 Results from D-FF-OCT observations of RA are presented in Figure 4. The three-dimensional
135 FF-OCT view of RA sporangiophores from Figure 4A confirms a length above 300 μm for
136 the longest and a diameter between 10 and 12 μm , without any septum. As for NG, the
137 dynamic D-OCT image from Figure 4B confirms a similar shape of the RA sporangiophores
138 with a homogenous and rather low dynamic contrast, from blue to pale green. Figure 4C
139 precisely shows the dotted spherical shape and organization of RA sporangium, with a total
140 diameter exceeding 100 μm . As for AF, the two-dimensional dynamic D-OCT image showing
141 RA sporangiospores seems to highlight two compartments within the sporangium, each with a
142 different contrast (Figure 4D): one in the center corresponding to the columellae, brighter and
143 with enhanced contrast when compared to a second more peripheral area unfolding all
144 sporangiospores.

145 4 Discussion

146 Except for a few reports describing the attempt to use standard OCT for the diagnosis of
147 onychomycosis [11], dermatophytoma [18] as well as other applications in ophthalmology
148 intended for the imaging of fungal keratitis [19] and chorioretinitis [20], there is to our
149 knowledge no report of high definition D-FF-OCT imaging in fungal diagnostics. Indeed, the
150 present study introduces the first observations of filamentous fungal species with D-FF-OCT,
151 demonstrating the complementary potential of both high-definition structure (Figures 2A, C,
152 Figure 3A and Figures 4A, C) and dynamic contrast (Figures 2B, D, Figures 3B, C and
153 Figures 4B, D) images for the identification of fungi.

154 First, FF-OCT acquisitions return comparable information regarding the global structure of all
155 three selected fungal species. In particular, the main characteristics of AF and RA with
156 conventional microscopy largely correspond to the one obtained with FF-OCT: the thin
157 branched and septate hyphae of AF (Figure 3A) are distinguishable from the larger pauci-
158 septate RA sporangiophores displaying a ribbon-like structure (Figure 4A). A similar
159 conclusion can be drawn from the comparison of AF conidial heads (Figure 3A) and the
160 dotted spherical organization of RA sporangiospores (Figure 4C) hiding two compartments
161 within the sporangium [6]. The observation of FF-OCT images of NG also confirms the
162 typical ellipsoidal and thin-walled structure of NG multicelled macroconidia (Figure 2C), as
163 for the usually reported microscopic examination and identification criteria [21]. Obviously,
164 these results need to be confirmed on other fungal species to test the global performances and
165 limits of such FF-OCT system for the identification of more precise morphological criteria
166 usually dedicated to microbiological diagnostics: notably information such as the number of
167 septa composing macroconidia or hyphae pigmentation.

168 In addition to such structural information, D-FF-OCT gave access to dynamic contrast
169 imaging of fungal cells. Briefly, this technology was previously shown to provide
170 complementary subcellular contrast to structural images obtained with FF-OCT. On the

171 suspected basis of mitochondria or cellular organelles movements, dynamic contrast has
172 already demonstrated its ability to reflect both cell activity and metabolism [8]. Interestingly,
173 the present data illustrate for the first time the exploitation of D-OCT to probe fungal
174 subcellular dynamics. As shown in Figures 2B and D, the comparison of hyphae and
175 macroconidia dynamic contrasts for NG very certainly reflects a different metabolic state of
176 both structures [22]. In the case of NG, the intense orange dynamic contrast within the
177 macroconidia may be the reflection of macroconidia metabolic activity (Figure 2D). Dynamic
178 D-OCT images of AF show the same kind of opposition between vesicles or certain
179 conidiophore segments displaying bright green-orange contrast and conidial heads or
180 phialides associated with a paler bluish signal (Figures 3B, C). As for MF, these dynamic
181 discrepancies in AF compartments very certainly correspond to a changing metabolic activity
182 and signature of each fungal structure, also possibly occurring in the center of RA sporangium
183 (Figure 4D). Still, additional experiments will be needed to better understand the exact nature
184 of such dynamic contrast. Indeed, live-cell imaging of filamentous fungi mainly relies on the
185 use of either cell wall or membrane selective dyes coupled with confocal laser scanning
186 microscopy to analyze subcellular compartments dynamics and provide a better understanding
187 of fungal morphogenesis [23,24]. A comparison of the signal obtained with D-OCT and live-
188 cell imaging would help to better understand the origin of D-OCT dynamic contrast in fungi.
189 Finally, given well known morphological discrepancies between *in vitro* and *in vivo* structural
190 or even metabolic characteristics of fungi, the present D-FF-OCT-based visualization of non-
191 dermatophytes filamentous species *in vitro* only constitutes the first attempt towards future
192 works to better appreciate the morphological aspect of the same molds *in vivo*, throughout
193 their parasitic phase, with deep-tissue D-FF-OCT imaging of direct clinical samples such as
194 cutaneous, mucosal or lung biopsy.

195 **5 Conclusion**

196 Overall, this study introduces a novel application of D-FF-OCT for fungal diagnostics. Based
197 on unprecedented structure and dynamic contrast imaging of three different fungal species, we
198 bring conclusive evidence that such technology not only allows rapid identification of fungal
199 compartments with a definition approaching conventional microscopy but also returns
200 potential precious metabolic information regarding fungal subcellular dynamics, without any
201 sample preparation, coloration, or any selective dye. Regarding clinical perspectives, it could
202 serve rapid bedside extemporaneous analysis following nail scraping, skin biopsy as well as
203 direct noninvasive *in vivo* histopathological examination of any skin or mucosal lesion within
204 a few minutes, potentially helpful when compared to the actual time constraints associated
205 with conventional preparations of histological sections (fixation, embedding, sectioning,
206 staining) that sometimes require days of technical procedures and lead to significant delay in
207 final diagnosis. Thus, we believe D-FF-OCT may serve as complementary tool for rapid IFI
208 diagnosis in future microbiological laboratory and clinical routine practice. Further studies are
209 needed to assess D-FF-OCT accuracy if applied to clinically relevant samples such as fresh
210 tissues.

211 **Figure captions**

212 Fig. 1. D-FF-OCT set up for the acquisition of fungal solid cultures. (A) Global view of both
213 hardware and software set up for fungal observations. (B) Fungal solid cultures exploited for
214 D-FF-OCT observations. (C) Frontal view of the D-FF-OCT acquisition system with sample
215 holder in the center. White arrow points the halogen source.

216 Fig. 2. D-FF-OCT observations of *Nannizzia gypsea*. (A) Two dimensional FF-OCT image
217 showing *Nannizzia gypsea* hyphae. (B) Two dimensional D-OCT image showing *Nannizzia*
218 *gypsea* hyphae. (C) Three dimensional FF-OCT image showing *Nannizzia gypsea* hyphae and
219 macroconidia. (D) Three dimensional D-OCT image showing *Nannizzia gypsea* hyphae and
220 macroconidia. Scale bar represents 50 μm . White arrow points the multicelled macroconidia.

221 Fig. 3. D-FF-OCT observations of *Aspergillus fumigatus*. (A) Two dimensional FF-OCT
222 image showing *Aspergillus fumigatus* conidiophore and conidial heads. (B) Two dimensional
223 D-OCT image showing *Aspergillus fumigatus* conidiophore and conidial heads. (C) Three
224 dimensional D-OCT image showing *Aspergillus fumigatus* conidiophore and conidial heads.
225 Scale bar represents 50 μm . White arrow points a conidial head of *Aspergillus fumigatus*.

226 Fig. 4. D-FF-OCT observations of *Rhizopus arrhizus*. (A) Three dimensional FF-OCT image
227 showing *Rhizopus arrhizus* sporangiophores. (B) Three dimensional D-OCT image showing
228 *Rhizopus arrhizus* sporangiophores. (C) Two dimensional FF-OCT image showing *Rhizopus*
229 *arrhizus* sporangium and sporangiospores. (D) Two dimensional D-OCT image showing
230 *Rhizopus arrhizus* sporangium and sporangiospores. Scale bar represents 50 μm .

231

232 **Conflict of Interest**

233 *The authors declare that the research was conducted in the absence of any commercial or*
234 *financial relationships that could be construed as a potential conflict of interest.*

235 **Author Contributions**

236 TM and MS designed the study, conducted experiments, performed experimental works and
237 wrote the manuscript. JMC, CB, DGH, FL and MS performed experimental works. JMC, CB,
238 MB, LP, DGH, FL, MS and PEC contributed to the manuscript revision. TM, MS and FD
239 supervised the project.

240 All authors contributed to the article and approved the submitted version.

241 **Funding**

242 This work was supported by crowdfunding (<https://thellie.org/mycoct>), by the WIFI labex and
243 the HELMHOLTZ SYNERGY ERC PROGRAM.

244 **Acknowledgments**

245 We sincerely thank Beclere Corentin, Choux Isabelle, De Tardy De Montrave Françoise,
246 Gitton Véronique, Laurenceau Raphaëlle, Vincent Anne and Bailly Eloïse for their help
247 regarding solid cultures of fungal species.

248 **Data Availability Statement**

249 All data from the study are included in the article. Further inquiries can be directed to the
250 corresponding author.

251 **References**

- 252 [1] Chowdhary A, Sharma C, Meis JF. Azole-Resistant Aspergillosis: Epidemiology,
253 Molecular Mechanisms, and Treatment. *The Journal of Infectious Diseases*
254 2017;216:S436–44. <https://doi.org/10.1093/infdis/jix210>.
- 255 [2] Danion F, Duréault A, Gautier C, Senechal A, Persat F, Bougnoux M-E, et al.
256 Emergence of azole resistant-*Aspergillus fumigatus* infections during STAT3-
257 deficiency. *Journal of Medical Microbiology* 2020;69:844–9.
258 <https://doi.org/10.1099/jmm.0.001200>.
- 259 [3] Donnelly JP, Chen SC, Kauffman CA, Steinbach WJ, Baddley JW, Verweij PE, et al.
260 Revision and Update of the Consensus Definitions of Invasive Fungal Disease From the
261 European Organization for Research and Treatment of Cancer and the Mycoses Study
262 Group Education and Research Consortium. *Clinical Infectious Diseases* 2020;71:1367–
263 76. <https://doi.org/10.1093/cid/ciz1008>.
- 264 [4] Pruskowski KA, Mitchell TA, Kiley JL, Wellington T, Britton GW, Cancio LC.
265 Diagnosis and Management of Invasive Fungal Wound Infections in Burn Patients. *EBJ*
266 2021;2:168–83. <https://doi.org/10.3390/ejb2040013>.
- 267 [5] Dekio F, Bhatti TR, Zhang SX, Sullivan KV. Positive Impact of Fungal Histopathology
268 on Immunocompromised Pediatric Patients With Histology-Proven Invasive Fungal
269 Infection. *Am J Clin Pathol* 2015;144:61–7.
270 <https://doi.org/10.1309/AJCPEMVYT88AVFKG>.
- 271 [6] Antinori S, Corbellino M, Parravicini C. Challenges in the Diagnosis of Invasive Fungal
272 Infections in Immunocompromised Hosts. *Curr Fungal Infect Rep* 2018;12:12–22.
273 <https://doi.org/10.1007/s12281-018-0306-0>.
- 274 [7] Quénéhervé L, Olivier R, Gora MJ, Bossard C, Mosnier J-F, Benoit a la Guillaume E, et
275 al. Full-field optical coherence tomography: novel imaging technique for
276 extemporaneous high-resolution analysis of mucosal architecture in human gut biopsies.
277 *Gut* 2021;70:6–8. <https://doi.org/10.1136/gutjnl-2020-321228>.
- 278 [8] Apelian C, Harms F, Thouvenin O, Boccara AC. Dynamic full field optical coherence
279 tomography: subcellular metabolic contrast revealed in tissues by interferometric signals
280 temporal analysis. *Biomed Opt Express* 2016;7:1511.
281 <https://doi.org/10.1364/BOE.7.001511>.
- 282 [9] Dalimier E, Salomon D. Full-Field Optical Coherence Tomography: A New Technology
283 for 3D High-Resolution Skin Imaging. *Dermatology* 2012;224:84–92.
284 <https://doi.org/10.1159/000337423>.
- 285 [10] Maldiney T, Greigert H, Martin L, Benoit E, Creuzot-Garcher C, Gabrielle P-H, et al.
286 Full-field optical coherence tomography for the diagnosis of giant cell arteritis. *PLoS*
287 *ONE* 2020;15:e0234165. <https://doi.org/10.1371/journal.pone.0234165>.
- 288 [11] Olsen J, Lindsø Andersen P, Themstrup L, Jemec GBE, Saunte DML. Optical coherence
289 tomography of onychomycosis: proposed terminology and a suggestion of practical
290 usage. *Arch Dermatol Res* 2020;312:51–8. <https://doi.org/10.1007/s00403-019-01989-8>.
- 291 [12] van Manen L, Dijkstra J, Boccara C, Benoit E, Vahrmeijer AL, Gora MJ, et al. The
292 clinical usefulness of optical coherence tomography during cancer interventions. *J*
293 *Cancer Res Clin Oncol* 2018;144:1967–90. <https://doi.org/10.1007/s00432-018-2690-9>.
- 294 [13] Andersen AJB, Fuchs C, Ardigo M, Haedersdal M, Mogensen M. In vivo
295 characterization of pustules in *Malassezia* Folliculitis by reflectance confocal

- 296 microscopy and optical coherence tomography. A case series study. *Skin Res Technol*
297 2018;24:535–41. <https://doi.org/10.1111/srt.12463>.
- 298 [14] Morsy H, Mogensen M, Thomsen J, Thrane L, Andersen PE, Jemec GBE. Imaging of
299 cutaneous larva migrans by optical coherence tomography. *Travel Medicine and*
300 *Infectious Disease* 2007;5:243–6. <https://doi.org/10.1016/j.tmaid.2006.12.004>.
- 301 [15] Banzhaf CA, Themstrup L, Ring HC, Welzel J, Mogensen M, Jemec GBE. In vivo
302 Imaging of *Sarcoptes scabiei* Infestation Using Optical Coherence Tomography. *Case*
303 *Rep Dermatol* 2013;5:156–62. <https://doi.org/10.1159/000352066>.
- 304 [16] Ghouali W, Grieve K, Bellefqih S, Sandali O, Harms F, Laroche L, et al. Full-Field
305 Optical Coherence Tomography of Human Donor and Pathological Corneas. *Current*
306 *Eye Research* 2015;40:526–34. <https://doi.org/10.3109/02713683.2014.935444>.
- 307 [17] Harris JL. Safe, low-distortion tape touch method for fungal slide mounts. *J Clin*
308 *Microbiol* 2000;38:4683–4. <https://doi.org/10.1128/JCM.38.12.4683-4684.2000>.
- 309 [18] Verne SH, Chen L, Shah V, Nouri K, Tosti A. Optical Coherence Tomography Features
310 of Dermatophytoma. *JAMA Dermatol* 2018;154:225.
311 <https://doi.org/10.1001/jamadermatol.2017.4590>.
- 312 [19] Sharma N, Singhal D, Maharana PK, Agarwal T, Sinha R, Satpathy G, et al. Spectral
313 Domain Anterior Segment Optical Coherence Tomography in Fungal Keratitis. *Cornea*
314 2018;37:1388–94. <https://doi.org/10.1097/ICO.0000000000001715>.
- 315 [20] Adam MK, Rahimy E. Enhanced Depth Imaging Optical Coherence Tomography of
316 Endogenous Fungal Chorioretinitis. *JAMA Ophthalmol* 2015;133:e151931.
317 <https://doi.org/10.1001/jamaophthalmol.2015.1931>.
- 318 [21] Mohamed Shalaby MF, Nasr El-din A, Abu El-Hamd M. Isolation, Identification, and In
319 Vitro Antifungal Susceptibility Testing of Dermatophytes from Clinical Samples at
320 Sohag University Hospital in Egypt. *Electron Physician* 2016;8:2557–67.
321 <https://doi.org/10.19082/2557>.
- 322 [22] Dill BC, Leighton TJ, Stock JJ. Physiological and biochemical changes associated with
323 macroconidial germination in *Microsporum gypseum*. *Appl Microbiol* 1972;24:977–85.
324 <https://doi.org/10.1128/am.24.6.977-985.1972>.
- 325 [23] Lichius A, Zeilinger S. Application of Membrane and Cell Wall Selective Fluorescent
326 Dyes for Live-Cell Imaging of Filamentous Fungi. *JoVE* 2019:60613.
327 <https://doi.org/10.3791/60613>.
- 328 [24] Pfister J, Lichius A, Summer D, Haas H, Kanagasundaram T, Kopka K, et al. Live-cell
329 imaging with *Aspergillus fumigatus*-specific fluorescent siderophore conjugates. *Sci Rep*
330 2020;10:15519. <https://doi.org/10.1038/s41598-020-72452-2>.
- 331

(A)

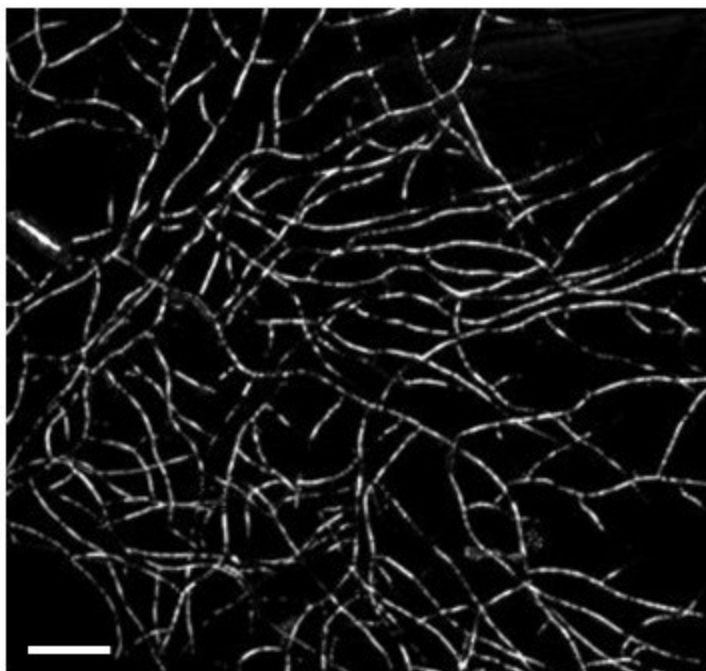
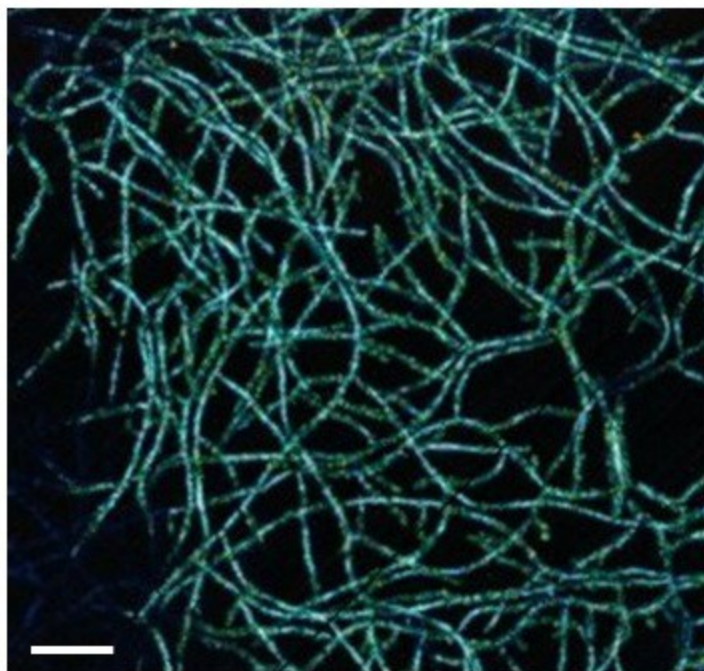
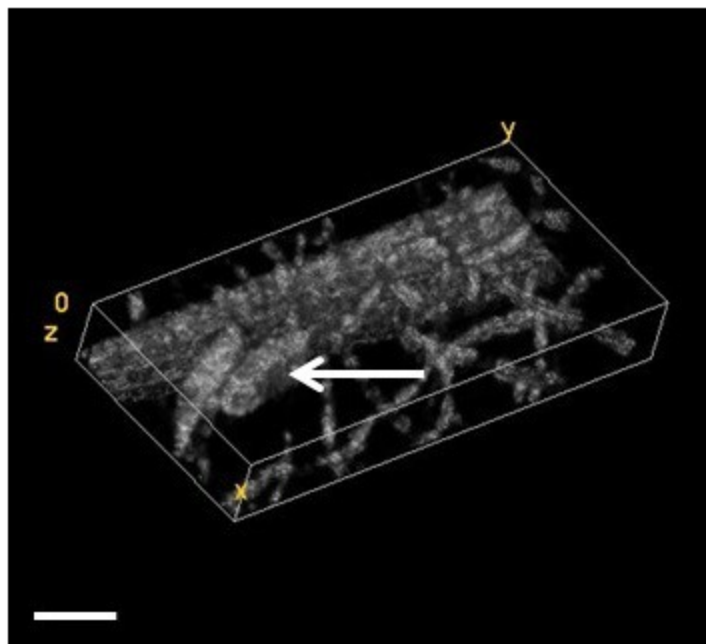
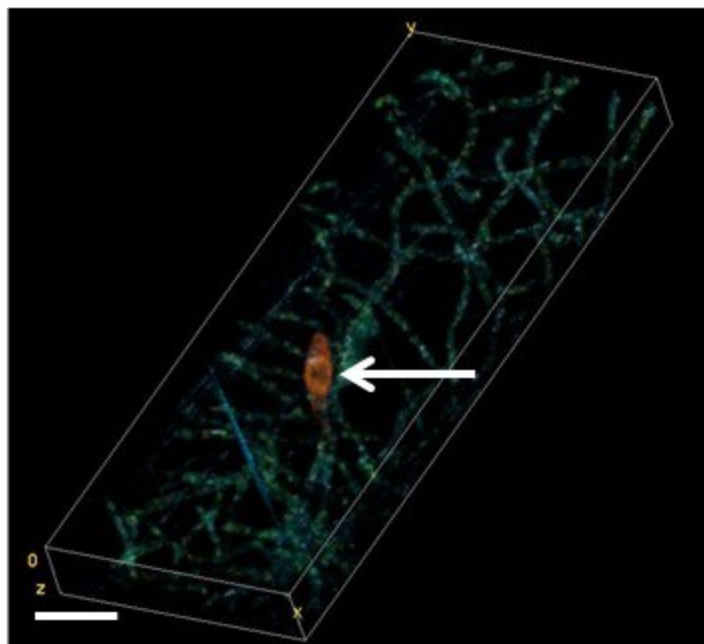


(B)

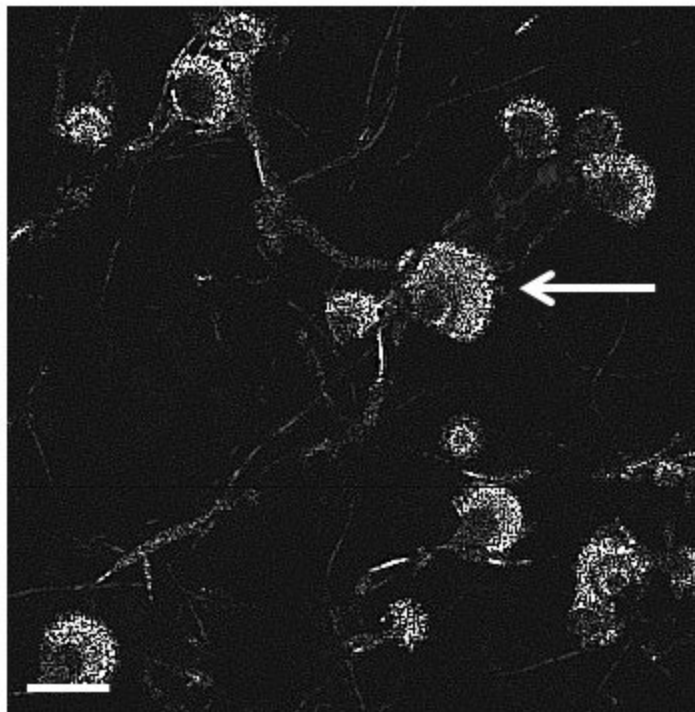


(C)

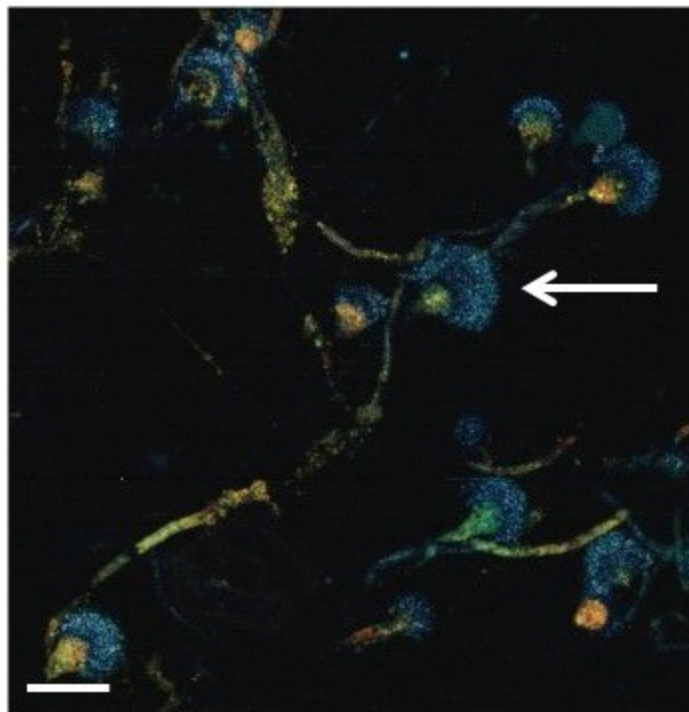


(A)**(B)****(C)****(D)**

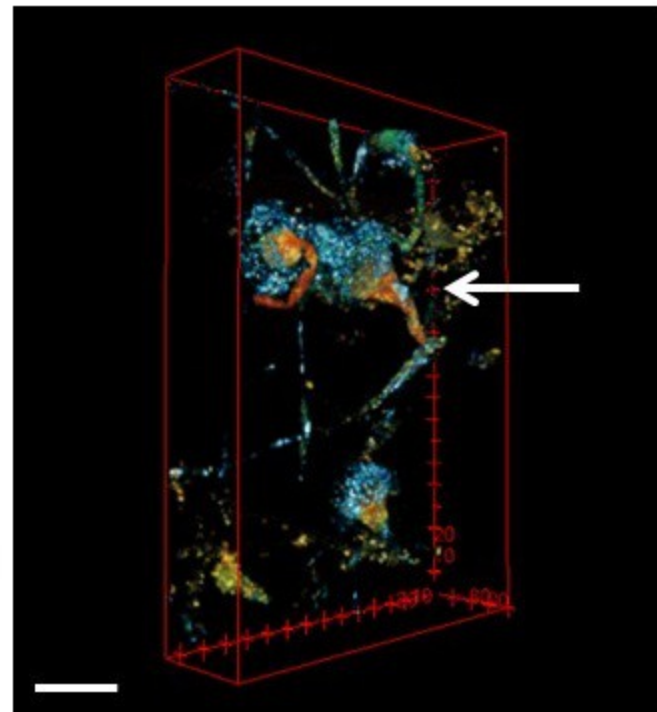
(A)

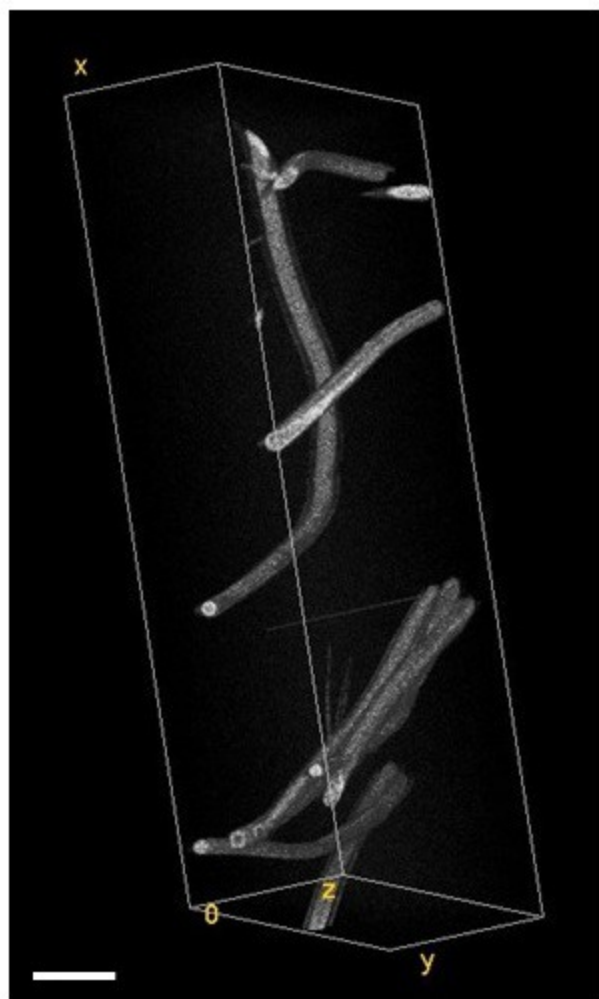
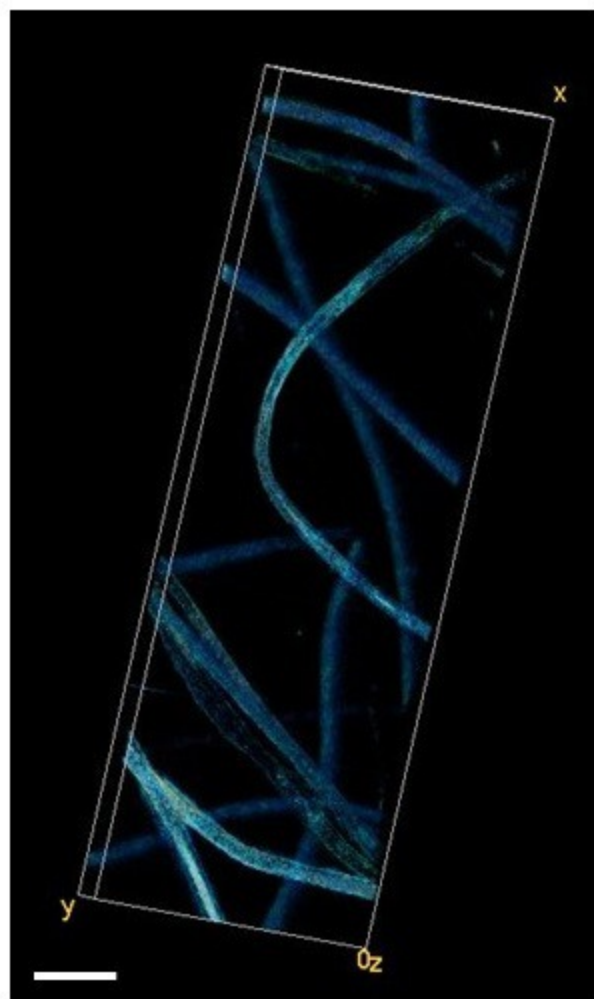
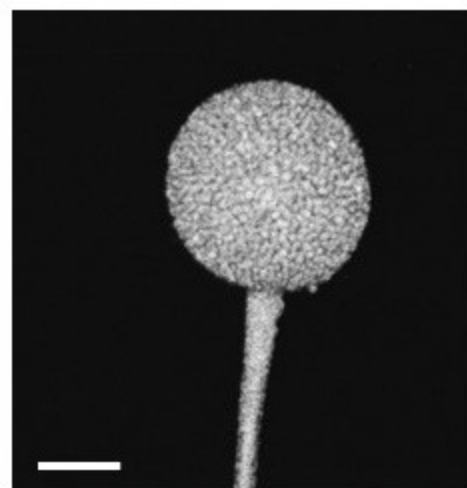


(B)



(C)



(A)**(B)****(C)****(D)**